JOURNAL OF SPACECRAFT AND ROCKETS
Vol. 44, No. 5, September–October 2007

Passive Stability Design for the Solar Sail on Displaced Orbits

Shengping Gong,* Junfeng Li,† and Hexi Baoyin‡
Tsinghua University, 100084 Beijing, People's Republic of China

DOI: 10.2514/1.29752

This paper investigates the passive stability design of a sailcraft on a displaced orbit with the orbit and attitude considered simultaneously. The objective is to stabilize the orbit-attitude coupled system passively by designing the sailcraft parameters. The design results show that the system can be marginally stable with passive control. First, the criteria for the passive stability of the sailcraft are given, and the coupled equations of motion are obtained. Then, the whole design problem is converted into an optimization problem by converting the design parameters into the optimization parameters, the static requirements of the stability criteria into constraints, and the dynamical requirements into the optimization function. Finally, an example of the optimal design is given. The simulation results under different initial conditions show that the sailcraft is marginally stable on the orbit.

Nomenclature

$\boldsymbol{F}_1$	=	resultant force of solar radiation pressure force exerted on S_1 and S_2, N
$\boldsymbol{F}_2$	=	resultant force of solar radiation pressure force exerted on S_3 and S_4, N
h_i	=	distance from apex to mass center of S_i, m
L	=	length of boom used to support the payload, m
m_b	=	mass of support bus, kg
m_p	=	mass of support payload, kg
m_s	=	mass of support bars, kg
$\boldsymbol{n}$	=	resultant force vector of solar radiation pressure, a unit vector
$\boldsymbol{n}_i$	=	unit normal vector of S_i, a unit vector
$\boldsymbol{n}_s$	=	unit normal vector of solar light, a unit vector
O	=	apex of cone formed by sails
Os	=	mass center of sailcraft
$O_s x_b y_b z_b$	=	body-fixed frame
$ox_o y_o z_o$	=	orbital frame
P_1	=	pressure center of S_1 and S_2
P_2	=	pressure center of S_3 and S_4
$\boldsymbol{r}_{AB}$	=	vector from point "A" to point "B," m
S_i	=	area of specific sail, m^2
z	=	displacement of displaced orbit, m
α	=	angle between resultant force vector of solar radiation pressure and solar light, rad
α_i	=	angle between solar light and normal vector of S_i, rad
β	=	lightness number of sail, dimensionless
γ_1	=	angle between S_1 and S_2, rad
γ_2	=	apex angle of S_1 and S_2, rad
γ_1'	=	angle between S_3 and S_4, rad
γ_2'	=	apex angle of S_3 and S_4, rad
η	=	angle between boom and x_b axis, rad
κ	=	weight coefficient in optimization function, dimensionless
μ	=	solar gravitational constant, m^3/s^2
ξ	=	characteristic index, dimensionless
ρ	=	radius of displaced orbit, m
σ	=	density of sail, kg/m^2
$\boldsymbol{\chi}$	=	$[\varphi\ \ \theta\ \ \psi]^T$, rad
ψ, ϕ, θ	=	yaw, pitch, and roll Euler angles, rad
$\boldsymbol{\omega}$	=	angular velocity vector of sailcraft, rad/s

Subscripts

b	=	projection of vector in body-fixed frame
o	=	projection of vector in orbital frame
0	=	quantity related to equilibrium point or reference displaced orbit

Received 19 January 2007; revision received 19 May 2007; accepted for publication 24 May 2007.

*Ph.D. Candidate, School of Aerospace; gsp04@mails.tsinghua.edu.cn.
†Professor, School of Aerospace; lijunf@tsinghua.edu.cn.
‡Associate Professor, School of Aerospace; baoyin@tsinghua.edu.cn. Member AIAA.

I. Introduction

RECENTLY, attention has been focused on solar sail missions, such as the new artificial Lagrange point created by solar sail to be used for NOAA/NASA/DOD (National Oceanic and Atmospheric Administration)/(U.S. Department of Defense) to provide early warning of solar plasma storms, before they reach Earth [1,2]. Sailcraft usually have a very large and complex structure, and conventional thrusters and reaction wheels are usually impractical or inefficient for the sailcraft control. Therefore, passive control is a good option; thus this paper investigates the passive stability of a sailcraft on a displaced solar orbit with the orbit and attitude considered simultaneously.

Displaced sailcraft orbits have been investigated for several years. In 1981, Forward [3] considered a displaced solar sail north or south of the geostationary ring. More recently, McInnes and Simmons [4] has done much work on the issue, in which large families of displaced orbits were investigated by considering the dynamics of a solar sail in a rotating frame. The dynamics, stability, and control of different families of displaced orbits were investigated in detail [5–9]. Molostov and Shvartsburg [10,11] investigated the displaced orbits when the solar sail with absorption was considered.

Attitude dynamics is another very important issue for solar sails. Attitude stabilization of a space vehicle by solar radiation pressure was first proposed by Sohn [12]. Since then, many researchers have investigated attitude stabilization of a satellite using solar radiation pressure. In fact, such a solar-pressure attitude control concept has been successfully implemented on a certain type of geostationary satellites as well as several interplanetary spacecraft. However, attitude control of a sailcraft is different from the solar-pressure attitude control for ordinary spacecraft. Recently, several attitude control strategies for solar sails have been proposed. The attitude dynamics and control of solar sails using a gimbaled control boom were investigated by Benjamin [13]. The gimbaled control boom and sail control vanes were discussed in detail in [14,15], and multiple simulations were given for various sail missions. In [16], the control system employs two ballast masses running along the mast for pitch/yaw control and roll stabilizer bars at the mast tips for quadrant tilt control. The second strategy employed a micropulsed plasma thruster mounted at the mast tips for attitude control. Passive control of an interplanetary spacecraft was discussed in [17] and passive control of the solar sail on the displaced solar orbit was investigated in [6]. The results from [6] show that the solar displaced orbits are stable if the sail pitch angle is fixed with respect to the rotating frame.

Most literatures dealt with the orbit and attitude of the solar sails separately. The attitude is usually investigated solely, and the orbit control is investigated with the assumption that the attitude can be adjusted freely to control the orbit. However, for the displaced orbits, the controlled attitude may lag behind the required attitude and that may make the orbit unstable. In addition, the deviation from the reference orbit will influence the attitude. Therefore, the orbital dynamics and attitude dynamics should be coupled to analyze the orbit stability.

In this paper, a sailcraft with a special configuration is discussed. Based on the presented configuration, the criteria of passive stability for the sailcraft on a displaced orbit are given. Then, the orbit-attitude coupled equations of motion for the solar sail are obtained. The coupled equations are linearized around the equilibrium solution to the equations and the stability of the equilibrium solution can be obtained by investigating the linear system. Last, the sailcraft parameters are designed to guarantee that the equilibrium point is stable. The results show that the orbit and attitude are both marginally stable with passive control.

II. Passive Stability Design Criteria

A four-triangle-form sail is adopted as the design model in this paper. Four isosceles triangles form a positive cone, four spars support the sails, and the spacecraft bus is positioned at the apex of the cone. The payload is located at the end of a massless boom, as shown in Fig. 1. The merit of the design is that the mounted payload can be used to perform active control when perturbations or solar activities drive the sailcraft off the nominal orbit.

The configuration of the sailcraft is shown in Figs. 1 and 2. The opposed triangle sails are designed with an equal apex angle, and match of the two sides of the adjacent triangles leads to the relations, given by

$$\gamma_1' = 2\sin^{-1}\left(\tan\frac{\gamma_2}{2} \Bigg/ \sqrt{\sec^2\frac{\gamma_2}{2} - \sin^2\frac{\gamma_1}{2}}\right) \tag{1}$$

$$\gamma_2' = 2\sin^{-1}\left(\sin\frac{\gamma_1}{2}\cos\frac{\gamma_2}{2}\right) \tag{2}$$

As given in [9], the lightness number of a sail is determined by its sail density σ (kg/m^2), as given by

$$\beta = \frac{1.53}{\sigma} \times 10^{-3} \tag{3}$$

As shown in Fig. 2, the two pressure centers P_1 and P_2 can be obtained by geometric relations, which are given in Eqs. (C6–C9). The resultant solar-pressure force exerted on the sailcraft can be given by

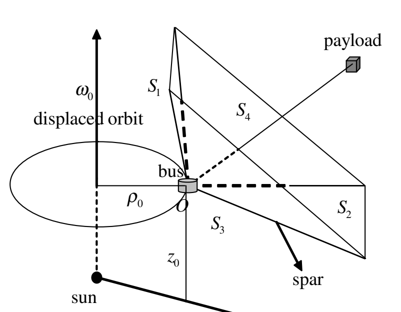

Fig. 1 Sailcraft on a displaced solar orbit.

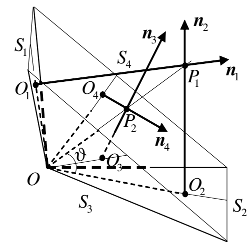

Fig. 2 Geometric parameters of the four sails.

$$\boldsymbol{F}_s = \boldsymbol{F}_1 + \boldsymbol{F}_2 \tag{4}$$

The expressions of $\boldsymbol{F}_1$ and $\boldsymbol{F}_2$ are given in Eqs. (B1) and (B2), respectively. The resultant torque relative to the center of mass can be given by

$$\boldsymbol{M}_{O_s} = \boldsymbol{r}_{O_sP_1} \times \boldsymbol{F}_1 + \boldsymbol{r}_{O_sP_2} \times \boldsymbol{F}_2 \tag{5}$$

The expression for $\boldsymbol{M}_{O_s}$ is given in Eq. (B5).

As discussed in [16,17], an interplanetary spacecraft is often considered to be statically stable when its center of mass lies between the sun and the center of the pressure. Passive stability means that, when the attitude is in an equilibrium position, the resultant solar-pressure force passes through the center of mass so that the resultant torque generated by the solar-pressure force is zero, and stabilizing torques are generated whenever the attitude deviates from the equilibrium position. For passive stability design, the attitude equilibrium position should be the attitude required to generate the orbit. Therefore, the force required by the orbit, denoted as $\boldsymbol{F}_r$, should be equal to the solar-pressure force generated by the sailcraft at the equilibrium position, that is, $\boldsymbol{F}_s = \boldsymbol{F}_r$. In addition, the solar-pressure torque relative to the center of mass should be zero when the attitude of the sail is in equilibrium position, that is, $\boldsymbol{M}_{O_s} = \boldsymbol{0}$.

The constraints $\boldsymbol{F}_s = \boldsymbol{F}_r$ and $\boldsymbol{M}_{O_s} = \boldsymbol{0}$ are the static requirements for the passive stability. To guarantee that the attitude equilibrium position is the attitude required to generate the orbit, the inertia of the sailcraft should be designed appropriately. Another requirement on the passive stability design is that, once the attitude or the orbit deviates from the equilibrium position, restoring forces and torques should be generated to stabilize the attitude and orbit. These requirements will be discussed in the following sections.

III. Displaced Solar Orbits

A displaced solar orbit is a circular sun-centered orbit displaced above the ecliptic plane by directing a component of the solar radiation pressure force in a direction normal to the ecliptic. For a single plane sail, the sail orientation is defined by its normal vector $\boldsymbol{n}$, fixed in the rotating frame, and the sailcraft performance is characterized by the sail lightness number β_0 [5]. As shown in Fig. 3, to keep an equilibrium in the rotating frame, the sail pitch angle α_0 and sail lightness β_0 for a displaced sun-centered orbit of radius ρ_0, displacement z_0, and orbital angular velocity $\boldsymbol{\omega}_0$ are given by [9]

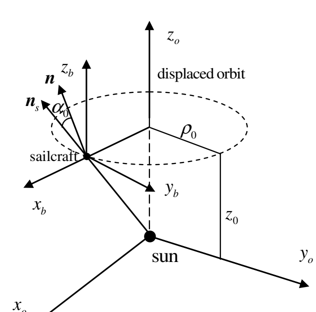

Fig. 3 Definition of reference frame.

$$\tan\alpha_0 = \frac{(z_0/\rho_0)(\omega_0/\tilde{\omega})^2}{(z_0/\rho_0)^2 + 1 - (\omega_0/\tilde{\omega})^2} \tag{6}$$

$$\beta_0 = [1 + (z_0/\rho_0)^2]^{\frac{1}{2}} \frac{\{(z_0/\rho_0)^2 + [1 - (\omega_0/\tilde{\omega})^2]^2\}^{\frac{3}{2}}}{[(z_0/\rho_0)^2 + 1 - (\omega_0/\tilde{\omega})^2]^2} \tag{7}$$

where $r_0^2 = \rho_0^2 + z_0^2$, and $\tilde{\omega}^2 = \mu/r_0^3$.

Here we define two frames, orbital frame $ox_oy_oz_o$ and body-fixed frame $O_sx_by_bz_b$. The origin of the orbital frame is the mass center of the sun; the x_o axis is in the elliptic plane and rotates around the sun with an angular velocity $\boldsymbol{\omega}_0$; the z_0 axis is in the direction of the angular velocity $\boldsymbol{\omega}_0$; and the y_o axis forms a right-handed triad. The origin of the body-fixed frame is the mass center of the sailcraft. When the sail is in equilibrium position, all the axes of the body-fixed frame are parallel to those of the orbital frame. The transformation between the two frames can be completed by three Euler rotations.

Assume that the opposed sails S_3 and S_4 are placed windward, as shown in Fig. 1. Because the required solar-pressure force lies in the plane spanned by $\boldsymbol{\omega}_0$ and $\boldsymbol{r}_0$, the sails S_3 and S_4 should be designed with equal area and placed symmetrically. However, no symmetric axis exists in the plane spanned by $\boldsymbol{\omega}_0$ and $\boldsymbol{r}_0$. Therefore, the opposed sails, denoted by S_1 and S_2, need to be either designed unequally or placed asymmetrically. The angle between $\boldsymbol{n}_s$ and the normal vector of S_i is denoted as α_i $(i = 1, 2, 3, 4)$. For the symmetry of the sailcraft, we have

$$S_3 = S_4 \tag{8}$$

$$\alpha_3 = \alpha_4 = \frac{\pi - \gamma_1'}{2} \tag{9}$$

$$\alpha_1 + \alpha_2 = \pi - \gamma_1 \tag{10}$$

The required solar-pressure force for a displaced solar orbit of radius ρ_0, displacement z_0, and orbital angular velocity $\boldsymbol{\omega}_0$ can be given by

$$\boldsymbol{F}_r = [\sigma(S_1 + S_1 + S_3 + S_4) + m_s + m_p + m_b]\frac{\beta_0\mu}{r_0^4}(\boldsymbol{n}\cdot\boldsymbol{r}_0)^2\boldsymbol{n} \tag{11}$$

The inertia of the sailcraft in the body-fixed frame is the summation of the inertia of every part of the sailcraft, given as $\boldsymbol{I} = \boldsymbol{I}_{\text{bus}} + \boldsymbol{I}_{\text{sail}} + \boldsymbol{I}_{\text{spar}} + \boldsymbol{I}_{\text{payload}}$. The detailed calculations of the inertia are presented in Appendix A. When the sailcraft is on a displaced orbit, the normal vectors of the sails should rotate once per orbit with respect to the inertial frame. To make sure that the equilibrium solution to the attitude equation of motion is the attitude required to generate the displaced orbit, the angular momentum of the sailcraft should be conserved when the sailcraft is revolving on the orbit. Therefore, the direction of the angular velocity should be parallel to one principle axis of the inertia. The sailcraft is symmetrical with respect to the plane spanned by $\boldsymbol{\omega}_0$ and $\boldsymbol{r}_0$. Therefore, only the nondiagonal element I_{xz} of the inertia is nonzero. In addition, the payload can be adjusted appropriately to make sure that the direction of the angular velocity is parallel to a principle axis, namely, $I_{xz} = 0$. The resultant solar-pressure force lies in the plane spanned by $\boldsymbol{\omega}_0$ and $\boldsymbol{r}_0$; thus the mass center of the sailcraft should lie in this plane. Therefore, the payload only needs to be adjusted in the plane. Then, two parameters L and η can be employed to determine the position of the payload, where L is the length of the massless boom and η determines the direction of the boom.

IV. Dynamical Attitude Equations

The relative orientation of the sailcraft, with respect to the orbital frame, is described by three Euler angles (φ, θ, ψ) of the rotational sequence of $R_2(\theta) \leftarrow R_1(\varphi) \leftarrow R_3(\psi)$ from the orbital frame to the body-fixed frame. The transition matrix can be given by

$$A = R_2(\theta)R_1(\varphi)R_3(\psi) \tag{12}$$

The angular velocity components of the sailcraft in frame $O_sx_by_bz_b$ can be given by

$$\boldsymbol{\omega}_b = \begin{bmatrix} \omega_x \\ \omega_y \\ \omega_z \end{bmatrix} = \begin{bmatrix} -\dot{\psi}s_\theta c_\varphi + \dot{\varphi}c_\theta \\ \dot{\psi}s_\varphi + \dot{\theta} \\ \dot{\psi}c_\theta c_\varphi + \dot{\varphi}s_\theta \end{bmatrix} + A\begin{bmatrix} 0 \\ 0 \\ \omega_0 \end{bmatrix} \tag{13}$$

Let $\boldsymbol{\chi} = [\varphi \;\; \theta \;\; \psi]^T$ and denote $\sin\theta$ and $\cos\theta$ by s_θ and c_θ, respectively. Then, the kinematical differential equation can be written as

$$\dot{\boldsymbol{\chi}} = \begin{bmatrix} \dot{\varphi} \\ \dot{\theta} \\ \dot{\psi} \end{bmatrix} = \frac{1}{c_\varphi}\begin{bmatrix} (\omega_x + \omega_0 c_\varphi s_\theta)c_\theta c_\varphi + (\omega_z - \omega_0 c_\varphi c_\theta)s_\theta c_\varphi \\ (\omega_x + \omega_0 c_\varphi s_\theta)s_\theta s_\varphi + (\omega_y - \omega_0 s_\varphi)c_\varphi - (\omega_z - \omega_0 c_\varphi c_\theta)c_\theta s_\varphi \\ -(\omega_x + \omega_0 c_\varphi s_\theta)s_\theta + (\omega_z - \omega_0 c_\varphi c_\theta)c_\theta \end{bmatrix} \tag{14}$$

The attitude equation of motion can be obtained as

$$\boldsymbol{I}\dot{\boldsymbol{\omega}}_b + \boldsymbol{\omega}_b \times (\boldsymbol{I}\boldsymbol{\omega}_b) = \boldsymbol{M}_{O_s} \tag{15}$$

where $\boldsymbol{I}$ is the inertia, and the expression of $\boldsymbol{M}_{O_s}$ is given in Eq. (B5). The subscript b denotes the projection of a vector in the body-fixed frame and o in the orbital frame. For passive stability design, $\{\varphi = 0,\ \theta = 0,\ \psi = 0\}$ is an equilibrium solution to the attitude equation.

For small Euler angles, the attitude equation can be linearized around the equilibrium point, given by

$$\ddot{\boldsymbol{\chi}} + J_1\dot{\boldsymbol{\chi}} + V_1\boldsymbol{\chi} = 0 \tag{16}$$

The coefficient matrices are given in Eqs. (B7), (B9), and (B11).

V. Coupled Attitude and Orbital Equations of Motion

As described previously, the sailcraft attitude will determine its orbit. When the stability and control of the orbit are analyzed, the attitude should be considered. On the other hand, the solar-pressure torque exerted on the sailcraft changes with the orbit of the sailcraft. Therefore, the orbit and attitude should be combined together to analyze the stability of the coupled system.

As discussed in previous literature, only a two-body problem is employed to analyze the dynamics of the sailcraft. Namely, only solar gravitational force and solar radiation pressure force are considered. Thus, the orbital equation can be given by

$$\ddot{\boldsymbol{r}}_o + 2\boldsymbol{\omega}_0 \times \dot{\boldsymbol{r}}_o + \boldsymbol{\omega}_0 \times (\boldsymbol{\omega}_0 \times \boldsymbol{r}_o) = \boldsymbol{f}(\boldsymbol{r}_o) + \boldsymbol{g}(\boldsymbol{r}_o, \boldsymbol{n}_o^i) \tag{17}$$

where $\boldsymbol{f}(\boldsymbol{r}_o)$ is the gravitational force of the sun, and $\boldsymbol{g}(\boldsymbol{r}_o, \boldsymbol{n}_o^i)$ is the solar-pressure force. Their expressions are given in Eqs. (B3) and (B4).

Now, the orbit-attitude coupled equations can be obtained by combining Eqs. (15) and (17)

$$\begin{cases} \ddot{\boldsymbol{r}}_o + 2\boldsymbol{\omega}_0 \times \dot{\boldsymbol{r}}_o + \boldsymbol{\omega}_0 \times (\boldsymbol{\omega}_0 \times \boldsymbol{r}_o) = \boldsymbol{f}(\boldsymbol{r}_o) + \boldsymbol{g}(\boldsymbol{r}_o, \boldsymbol{n}_o^i) \\ \boldsymbol{I}\dot{\boldsymbol{\omega}}_b + \boldsymbol{\omega}_b \times (\boldsymbol{I}\boldsymbol{\omega}_b) = \boldsymbol{M}_{O_s} \end{cases} \tag{18}$$

The kinematical equation for the attitude equation is given by Eq. (14).

The normal vector of each triangle sail, which is a constant vector in the body-fixed frame, can be expressed in the orbital frame as

$$\boldsymbol{n}_o^i = A^T\boldsymbol{n}_b^i \qquad (i = 1, 2, 3, 4) \tag{19}$$

The solar-pressure direction $\boldsymbol{n}_s$, which is related to the position vector of the sailcraft, can be expressed in the body-fixed frame as

$$\boldsymbol{n}_b^s = A\boldsymbol{n}_o^s \tag{20}$$

In the coupled equations, the orbital equation includes the attitude information $\boldsymbol{n}_o^i$, and the attitude equation includes the orbital information r and $\boldsymbol{n}_b^s$. Therefore, it can be concluded that the attitude and orbit are closely coupled.

For the passive stability design, $\{\boldsymbol{r}_o^0 = [\rho_0 \;\; 0 \;\; z_0]^T, \boldsymbol{\chi}_0 = \boldsymbol{0}\}$ is an equilibrium solution to the coupled equations. The coupled equations can be linearized around the equilibrium point, and the linear equations can be obtained by perturbing the sail from its nominal orbit and attitude. A perturbation $\boldsymbol{\delta}$ is added to the sail position vector and $\boldsymbol{\chi}$ is added to the Euler angles such that $\boldsymbol{r}_o = \boldsymbol{r}_o^0 + \boldsymbol{\delta}$ and $\boldsymbol{\chi} = \boldsymbol{\chi}_0 + \boldsymbol{\chi}$. Then, the linear variational equations can be obtained as

$$\begin{cases} \ddot{\boldsymbol{\delta}} + J\dot{\boldsymbol{\delta}} + V\boldsymbol{\delta} + L\boldsymbol{\chi} = 0 \\ \ddot{\boldsymbol{\chi}} + J_1\dot{\boldsymbol{\chi}} + V_1\boldsymbol{\chi} + L_1\boldsymbol{\delta} = 0 \end{cases} \tag{21}$$

The coefficient matrices are given in Eqs. (B6–B11). They are determined by the value of the equilibrium point. Since the body-fixed frame and orbital frame are consistent with each other at the equilibrium point, all the vectors can be expressed either in an orbital frame or in a body-fixed frame. The projections of the vectors in these two frames are given in Appendix C.

The stability of the system can be obtained by checking the eigenvalues of the coefficient matrix, given by

$$C = \begin{bmatrix} 0_{3\times3} & E_{3\times3} & 0_{3\times3} & 0_{3\times3} \\ -V_1 & -J_1 & -L_1 & 0_{3\times3} \\ 0_{3\times3} & 0_{3\times3} & 0_{3\times3} & E_{3\times3} \\ -L & 0_{3\times3} & -V & -J \end{bmatrix} \tag{22}$$

where $E_{3\times3}$ and $0_{3\times3}$ are the unit matrix and zero matrix, respectively.

To quantify the stability or instability of the system, the parameter ξ, termed as the characteristic index, is defined as the maximal real part of all the eigenvalues, that is, $\xi = \max_{1\le i\le 12}\mathrm{Re}(\lambda_i)$. If $\xi < 0$, the system is asymptotically stable and a smaller ξ means a faster stable transient response. If $\xi = 0$, the system is marginally stable . If $\xi > 0$, the system is unstable and a larger ξ means a faster divergent response.

VI. Passive Stability Design

According to the passive stability design criteria, the resultant solar-pressure force $\boldsymbol{F}_s$, resultant solar torque M_{O_s} and the nondiagonal element of the inertia I_{xz} should satisfy the constraints given by

$$\begin{cases} \boldsymbol{F}_s = \boldsymbol{F}_r \\ \boldsymbol{M}_{O_s} = \boldsymbol{0} \\ I_{xz} = 0 \end{cases} \tag{23}$$

Equation (23) guarantees that the equilibrium solution to the attitude equation is the attitude required to generate the displaced orbit, which is the static requirement. Another dynamical requirement is that stabilizing torques or forces will be generated if the attitude or the orbit deviates from the equilibrium position. For the design proposed in this paper, three rotations are coupled. If the design is not appropriate, the restoring torque generated in one direction may be counteracted by the torque generated in another one. Besides, even if the attitude is passively stabilized by the restoring torque, the orbit may be unstable, because the orbital stability relies not only on the attitude, but also on the displaced orbit size and the sailcraft configuration.

The objective of the passive stability design is to optimize the design parameters so as to minimize the characteristic index. However, the system cannot be made asymptotically stable using passive control. Therefore, the optimal result for the dynamical requirement is that ξ is minimized to zero (marginal stability). The design parameters related to the sailcraft are given as follows: the area of the triangle sails S_1, S_2, and S_3; the apex angle of the triangle sail γ_1; the angle between the opposed sails γ_2; the parameters determining the position of the payload L and η; the parameter determining the attitude of the sailcraft α_1.

The solution space for the design parameters is not null. Therefore, the sail area can be optimized when the sailcraft is passively stable. With the sail area to be optimized, the objective function can be written as

$$J = \xi + \kappa\sum_{i=1}^{4} S_i \tag{24}$$

where κ is a weight coefficient and should be chosen appropriately. If κ is too large, the system may be unstable. Otherwise, the sail area cannot be optimized to be minimal.

Now, the design problem can be converted into an optimization problem as stated: find optimal parameters $\boldsymbol{Y} = [S_1 \;\; S_2 \;\; S_3 \;\; \gamma_1 \;\; \gamma_2 \;\; l \;\; \eta \;\; \alpha_1]^T$ that minimize J subject to equality constraints given by Eq. (23). For the design problem in this paper, many local optimal solutions exist for the design parameters. For local optimization methods, the solution is dependent on the initial values of the parameters and it converges easily to the local optimal solution. Genetic algorithms are a global optimization method and can usually avoid local optimal solutions. Therefore, a genetic algorithm is employed to solve the optimization problem in this paper.

VII. Numerical Simulations

The simulated displaced solar orbit is an Earth-synchronous orbit with $\rho_0 = 0.98$ AU and $z_0 = 0.001$ AU (astronomical unit). The lightness β_0 and pitch angle α_0 required to generate the orbit can be obtained from Eqs. (6) and (7). The parameters related to the sailcraft are given in Table 1.

The simulated sailcraft is designed with four congruent triangle sails. Then, the geometric parameters γ_2, γ_2', and γ_1' are determined by γ_1. Therefore, the optimization parameters are reduced to $\boldsymbol{Y} = [S_1 \;\; \gamma_1 \;\; l \;\; \eta \;\; \alpha_1]^T$. The results of optimal parameters and objective function are listed in Table 2.

The optimized system is essentially marginally stable because the maximum real part of the eigenvalues is zero, and all the eigenvalues are six pairs of pure imaginary roots, given by $\lambda_{1,2} = \pm j1.25(10^{-3})$, $\lambda_{3,4} = \pm j1.25(10^{-3})$, $\lambda_{5,6} = \pm j1.99(10^{-7})$, $\lambda_{7,8} = \pm j1.99(10^{-7})$, $\lambda_{9,10} = \pm j2.59(10^{-8})$, and $\lambda_{11,12} = \pm j5.92(10^{-10})$. When all parameters related to the sailcraft have been obtained, the coupled dynamics of the sailcraft on the displaced orbit can be investigated. The nonlinear coupled equations of motion given by Eq. (18) and the kinematical equation given by Eq. (14) are employed to investigate the attitude and orbit responses.

Instead of x_o and y_o, the radius in ox_oy_o plane, $\rho_o = \sqrt{x_o^2 + y_o^2}$, is employed to analyze the orbital stability. The coupled equations are

Table 1 Sailcraft parameters

Parameters	Value
Sail density (σ)	0.01 kg/m^2
Bus	50 kg
Payload	20 kg
Density of support spars	0.1191 kg/m

Table 2 Optimal parameters

Parameters	Value
S_1	1531.54 m^2
γ_1	162.95 deg
L	79.17 m
η	180.00 deg
α_1	8.43 deg
ξ	3.90(10^{-20})

Table 3 Initial simulation errors

Case	$\delta\phi$, rad	$\delta\theta$, rad	$\delta\psi$, rad	δx, km	δy, km	δz, km
A	1×10^{-5}	1×10^{-5}	1×10^{-5}	0	0	0
B	1×10^{-3}	1×10^{-3}	1×10^{-3}	0	0	0
C	0	0	0	1×10^{3}	1×10^{3}	1×10^{3}
D	0	0	0	1×10^{5}	1×10^{5}	1×10^{5}
E	1×10^{-3}	1×10^{-3}	1×10^{-3}	1×10^{5}	1×10^{5}	1×10^{5}

integrated numerically with different initial orbital errors and attitude errors. Five groups of initial values, labeled as groups A, B, C, D, and E, are used to investigate the orbital stability of the sailcraft with passive stability design parameters. The initial errors for each group are given in Table 3.

The simulation results are presented in Figs. 4–9. The pitch angle responses, roll angle responses, yaw angle responses, radii responses, and displacement responses are presented in Figs. 4–8, while the orbits projected in the inertial frame are presented in Fig. 9. The responses of the attitude include multifrequency components because all the eigenvalues of the coefficient matrix are pure imaginary numbers. Therefore, the responses of different time spans are shown to illustrate the oscillations of different periods. The high-frequency oscillations with a period of about 85 min are related to the eigenvalues $\lambda_{1,2}$ and $\lambda_{3,4}$, which can be observed from the oscillations during the first day, as shown in the left columns in Figs. 4–6. The long-period oscillations with a period of about 1 year are related to the eigenvalues $\lambda_{5,6}$ and $\lambda_{7,8}$, which can be observed from the oscillations during the first 1000 days, as shown in the

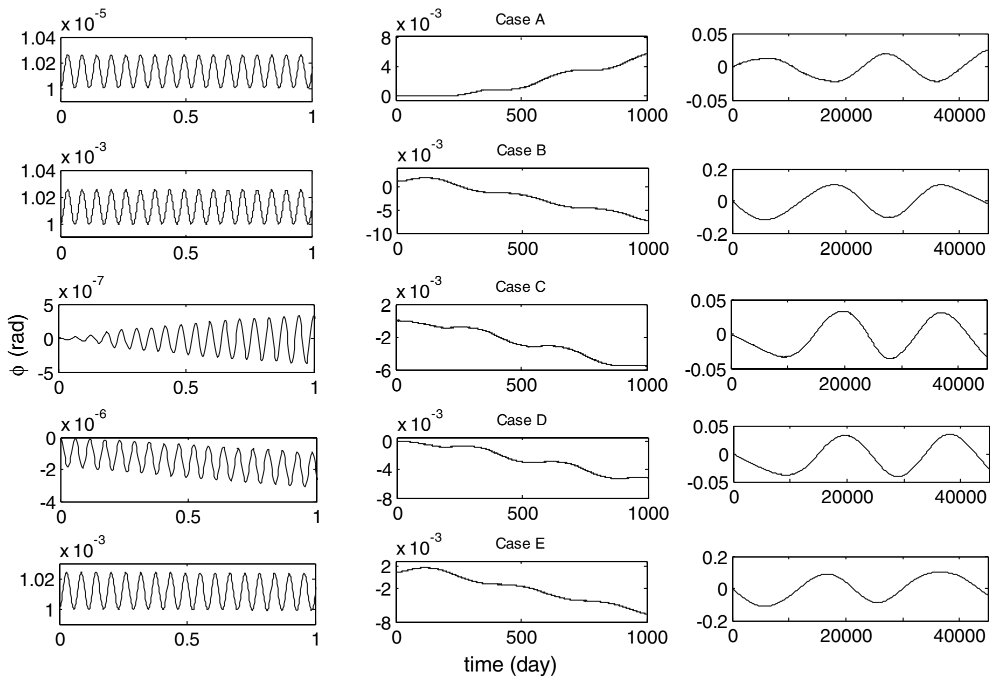

Fig. 4 Pitch angle responses for different initial errors.

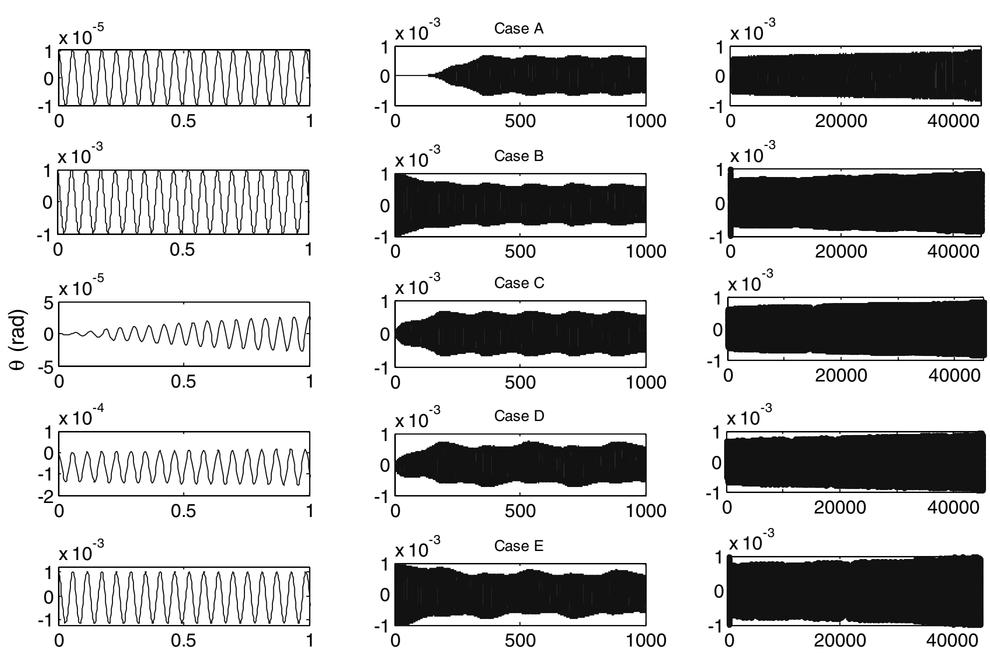

Fig. 5 Roll angle responses for different initial errors.

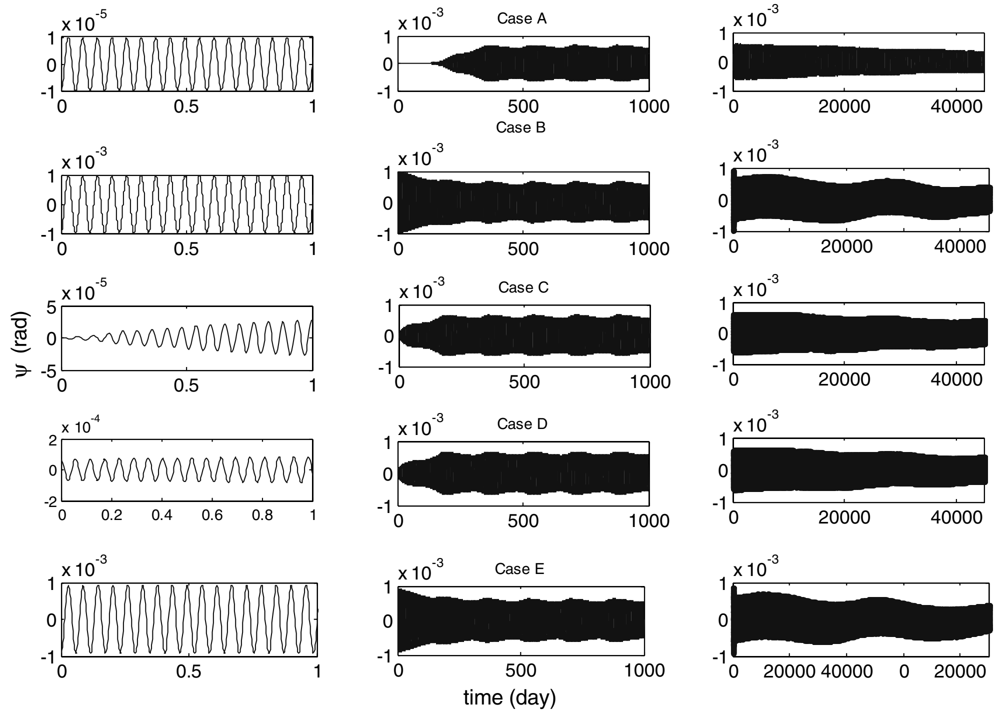

Fig. 6 Yaw angle responses for different initial errors.

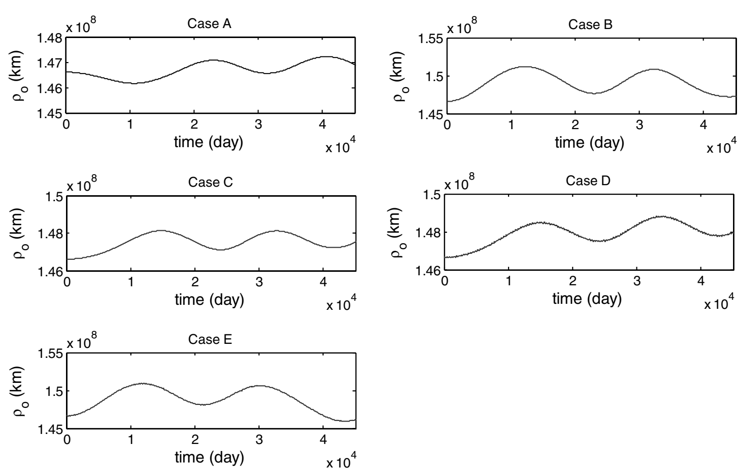

Fig. 7 Responses of orbital radius for different initial errors.

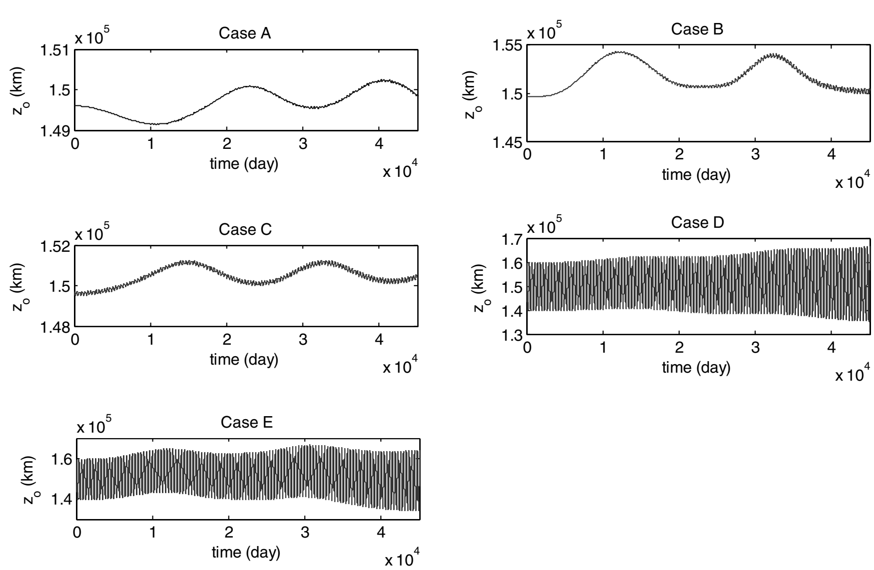

Fig. 8 Responses of orbital displacement for different initial errors.

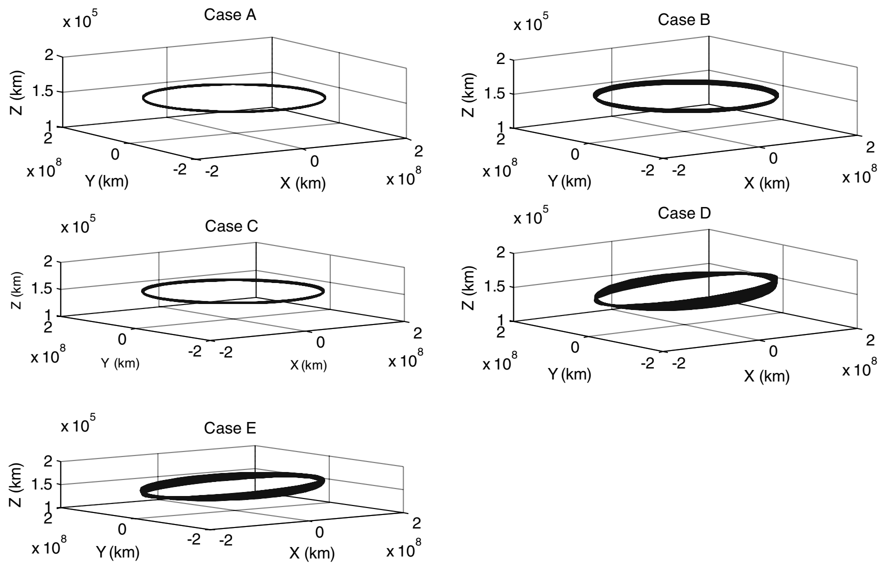

Fig. 9 Displaced orbits expressed in the inertial frame.

middle columns of Figs. 4–6. The long-period oscillations with a period of about 30,000 days are related to the eigenvalues $\lambda_{9,10}$, which can be observed from long responses during about 45,000 days, as shown in the right columns of Figs. 4–6.

From Fig. 4, it can be found that the pitch angle oscillates in the vicinity of the equilibrium position. Because the rotation axis of the pitch angle is close to the symmetrical axis of the cone formed by the four sails, the forces and torques generated by the solar radiation pressure are not very sensitive to the changes of the pitch angle. When the pitch angle is small, the restoring torques are always counteracted by the torques generated by other attitude angle errors. Therefore, the pitch angle needs larger amplitude to obtain enough restoring torques.

The responses of the roll and yaw angles are given in Figs. 5 and 6, respectively. Compared with the amplitude of the pitch angle, the amplitudes of the two attitude angles are rather small because the forces and torques are very sensitive to the variations of the two attitude angles, and small angles will generate enough restoring forces and torques. The results presented by the figures show that the amplitudes of different simulations are about 10^{-3} rad, and the amplitudes are almost invariant with the initial errors.

From the radii responses in Fig. 7, it can be concluded that both the initial attitude and orbital errors lead to the radii oscillations and the oscillation amplitudes increase as either the initial attitude errors or the initial orbital errors increase. The displacement responses are shown in Fig. 8. Similarly, the oscillation amplitudes also increase with the initial errors.

Last, the orbits for each case in the inertial frame are shown in Fig. 9. When the initial errors are small, the orbit is almost periodic, as shown in case A. As the initial errors increase, the trajectory of the sailcraft becomes a belt around the displaced orbit, instead of a circular orbit. The belt ranges increase with initial errors, as shown in cases A–E. From the simulation results, it can be concluded that, with small perturbations, the sailcraft is marginally stable on the orbit.

VIII. Conclusions

The criteria of passive stability include static and dynamical requirements. For the static requirements, the equilibrium position of the attitude should be the attitude required to generate the orbit. For the dynamical requirements, whenever the attitude or orbit deviates from its equilibrium position, restoring torques and forces should be generated to stabilize the attitude and orbit.

A four-triangle-form sail is investigated in this study. According to the design criteria of passive stability, the design problem is converted into an optimization problem. Based on the optimal design parameters obtained from the optimization method, the coupled dynamics of the sailcraft are investigated with different initial values. The simulation results show that the attitude angles oscillate around the equilibrium point, and the oscillation amplitude increases with the initial errors. The oscillation amplitudes of the roll and yaw angles are almost independent of the initial values. The orbital responses are similar to pitch angle responses, in that they oscillate around the equilibrium point and the amplitudes increase with initial errors. Therefore, to reduce the amplitudes of the oscillations, the initial errors should be as small as possible.

Appendix A: Inertia Calculations

The inertia of a triangle sail, with an area of S and apex angle of γ, can be calculated in the frame defined as follows: the origin is the mass center of the sail; the x axis points from mass center to the apex; the z axis is perpendicular to the sail; and the y axis forms a right-hand triangle. The edge of the triangle is given by

$$l = \sqrt{\frac{2S}{\sin\gamma}} \tag{A1}$$

The distance from the apex to the mass center can be written as

$$h = \frac{\int x\,\mathrm{d}s}{S} = \frac{\int_0^{l\cos\gamma}\int_{-\tan\frac{\gamma}{2}x}^{\tan\frac{\gamma}{2}x} x\,\mathrm{d}x\,\mathrm{d}y}{\frac{1}{2}l^2\sin\gamma} = \frac{4}{3}\tan\frac{\gamma}{2}\cos^3\frac{\gamma}{2}\,l/\sin\gamma \tag{A2}$$

Then, the inertia of the sail is obtained as

$$I_{sx} = \int (y^2+z^2)\,\mathrm{d}m = \frac{\sigma}{6}\tan^3\frac{\gamma}{2}\left[h^4 - \left(h - l\cos\frac{\gamma}{2}\right)^4\right] \tag{A3}$$

$$\begin{aligned} I_{sy} &= \int (x^2+z^2)\,\mathrm{d}m \\ &= 2\sigma\tan\frac{\gamma}{2}\left[\frac{h^4}{12} + \left(l\cos\frac{\gamma}{2} - h\right)^3\left(\frac{h}{12} + \frac{l}{4}\cos\frac{\gamma}{2}\right)\right] \end{aligned} \tag{A4}$$

$$I_{sz} = \int (x^2+y^2)\,\mathrm{d}m = I_{sx} + I_{sy} \tag{A5}$$

$$I_{sxy} = I_{sxz} = I_{syz} = 0 \tag{A6}$$

The transition matrixes, from the body-fixed frame to the frame as defined by the principle axis of inertia, are labeled as A_{S_1}, A_{S_2}, A_{S_3}, and A_{S_4}. They can be written as

$$A_{S_1} = R_2\left(\frac{\pi}{2} - \alpha_1 - \gamma\right) \tag{A7}$$

$$A_{S_2} = R_2\left(\frac{3\pi}{2}\alpha - \gamma - \alpha_2\right) \tag{A8}$$

$$A_{S_3} = R_3\left(\frac{\pi}{2}\right) R_1\left(\frac{\gamma_1' - \pi}{2}\right) R_2\left(\alpha_1 + \frac{\gamma_1}{2} - \gamma\right) \tag{A9}$$

$$A_{S_4} = R_3\left(-\frac{\pi}{2}\right) R_1\left(\frac{\pi - \gamma_1'}{2}\right) R_2\left(\alpha_1 + \frac{\gamma_1}{2} - \gamma\right) \tag{A10}$$

The mass centers of the four sails are labeled as O_1, O_2, O_3, and O_4. The mass center vectors of the four sails, relative to the mass center of the sailcraft, are expressed as $\boldsymbol{r}_{O_sO_1}$, $\boldsymbol{r}_{O_sO_2}$, $\boldsymbol{r}_{O_sO_3}$, and $\boldsymbol{r}_{O_sO_4}$. Then, the inertia of the four sails in the body-fixed frame can be given as

$$\begin{aligned} \boldsymbol{I}_{\text{sail}} = {} & A_{S_1}^T \boldsymbol{I}_s A_{S_1} + \sigma S_1\left(|\boldsymbol{r}_{O_sO_1}|^2 E_{3\times 3} - \boldsymbol{r}_{O_sO_1} \cdot \boldsymbol{r}_{O_sO_1}^T\right) + A_{S_2}^T \boldsymbol{I}_s A_{S_2} \\ & + \sigma S_2\left(|\boldsymbol{r}_{O_sO_2}|^2 E_{3\times 3} - \boldsymbol{r}_{O_sO_2} \cdot \boldsymbol{r}_{O_sO_2}^T\right) + A_{S_3}^T \boldsymbol{I}_s A_{S_3} \\ & + \sigma S_3\left(|\boldsymbol{r}_{O_sO_3}|^2 E_{3\times 3} - \boldsymbol{r}_{O_sO_3} \cdot \boldsymbol{r}_{O_sO_3}^T\right) + A_{S_4}^T \boldsymbol{I}_s A_{S_4} \\ & + \sigma S_4\left(|\boldsymbol{r}_{O_sO_4}|^2 E_{3\times 3} - \boldsymbol{r}_{O_sO_4} \cdot \boldsymbol{r}_{O_sO_4}^T\right) \end{aligned} \tag{A11}$$

For the support spars, the frame, as determined by the principle axis of inertia, can be defined as folows: the origin is the mass center of the spar; the z axis is along the spar; and the x and y axes are in the plane perpendicular to the z axis. The inertia of the spar in the frame can be obtained as

$$\boldsymbol{I}_B = \frac{1}{12} m_{\text{spar}} l^2 \begin{bmatrix} 1 & 0 & 0 \\ 0 & 1 & 0 \\ 0 & 0 & 0 \end{bmatrix} \tag{A12}$$

where m_{spar} is the mass of the spar, and l is the length of the spar.

The transition matrixes from the frame defined by the principle axis of inertia to the body-fixed frame are labeled as A_{B_1}, A_{B_2}, A_{B_3}, and A_{B_4}. They can be written as

$$A_{B_1} = R_2(\gamma_1 + \gamma + \alpha_2 - \pi) R_1\left(-\frac{\gamma_2}{2}\right) \tag{A13}$$

$$A_{B_2} = R_2(\gamma_1 + \gamma + \alpha_2 - \pi) R_1\left(\frac{\gamma_2}{2}\right) \tag{A14}$$

$$A_{B_3} = R_2(\pi - \gamma - \alpha_2) R_1\left(-\frac{\gamma_2}{2}\right) \tag{A15}$$

$$A_{B_4} = R_2(\pi - \gamma - \alpha_2) R_1\left(\frac{\gamma_2}{2}\right) \tag{A16}$$

The mass centers of the four spars are labeled as B_1, B_2, B_3, and B_4. The mass center vectors of the four spars, relative to the mass center of the sailcraft, are expressed as $\boldsymbol{r}_{O_sB_1}$, $\boldsymbol{r}_{O_sB_2}$, $\boldsymbol{r}_{O_sB_3}$, and $\boldsymbol{r}_{O_sB_4}$. Then, the inertia of the four spars in the body-fixed frame can be given as

$$\begin{aligned} \boldsymbol{I}_{\text{spar}} = {} & A_{B_1} \boldsymbol{I}_B A_{B_1}^T + m_{\text{spar}}\left(|\boldsymbol{r}_{O_sB_1}|^2 E_{3\times 3} - \boldsymbol{r}_{O_sB_1} \cdot \boldsymbol{r}_{O_sB_1}^T\right) \\ & + A_{B_2} \boldsymbol{I}_B A_{B_2}^T + m_{\text{spar}}\left(|\boldsymbol{r}_{O_sB_2}|^2 E_{3\times 3} - \boldsymbol{r}_{O_sB_2} \cdot \boldsymbol{r}_{O_sB_2}^T\right) \\ & + A_{B_3} \boldsymbol{I}_B A_{B_3}^T + m_{\text{spar}}\left(|\boldsymbol{r}_{O_sB_3}|^2 E_{3\times 3} - \boldsymbol{r}_{O_sB_3} \cdot \boldsymbol{r}_{O_sB_3}^T\right) \\ & + A_{B_4} \boldsymbol{I}_B A_{B_4}^T + m_{\text{spar}}\left(|\boldsymbol{r}_{O_sB_4}|^2 E_{3\times 3} - \boldsymbol{r}_{O_sB_4} \cdot \boldsymbol{r}_{O_sB_4}^T\right) \end{aligned} \tag{A17}$$

The inertia of the bus and the payload in the body-fixed can be expressed as

$$\boldsymbol{I}_{\text{bus}} = m_b \boldsymbol{r}_{O_sO_b} \boldsymbol{r}_{O_sO_b}^T \tag{A18}$$

$$\boldsymbol{I}_{\text{payload}} = m_p \boldsymbol{r}_{O_sO_p} \boldsymbol{r}_{O_sO_p}^T \tag{A19}$$

where $\boldsymbol{r}_{O_sO_b}$ and $\boldsymbol{r}_{O_sO_p}$ are mass center vectors of the sailcraft to the bus and payload, respectively.

The inertia of the sailcraft is the summation of the inertia of each part, as given by

$$\boldsymbol{I} = \boldsymbol{I}_{\text{sail}} + \boldsymbol{I}_{\text{spar}} + \boldsymbol{I}_{\text{payload}} + \boldsymbol{I}_{\text{bus}} \tag{A20}$$

Appendix B: Quantity Expressions

The solar radiation force exerted on the sails can be given by

$$\boldsymbol{F}_1 = \sigma S_1 \frac{\beta\mu(\boldsymbol{n}_1 \cdot \boldsymbol{n}_s)^2}{r^2} \boldsymbol{n}_1 + \sigma S_2 \frac{\beta\mu(\boldsymbol{n}_2 \cdot \boldsymbol{n}_s)^2}{r^2} \boldsymbol{n}_2 \tag{B1}$$

$$\boldsymbol{F}_2 = \sigma S_3 \frac{\beta\mu(\boldsymbol{n}_3 \cdot \boldsymbol{n}_s)^2}{r^2} \boldsymbol{n}_3 + \sigma S_4 \frac{\beta\mu(\boldsymbol{n}_4 \cdot \boldsymbol{n}_s)^2}{r^2} \boldsymbol{n}_4 \tag{B2}$$

where r is the distance from the sail to the sun.

The items related to the equation of motion are given by

$$f(\boldsymbol{r}_o) = -\frac{\mu}{r^3} \boldsymbol{r}_o \tag{B3}$$

$$\begin{aligned} g(\boldsymbol{r}_o, \boldsymbol{n}_o^i) = {} & \left[\sigma S_1 \frac{\beta_0\mu(\boldsymbol{n}_o^1 \cdot \boldsymbol{r}_o)^2}{r^4} \boldsymbol{n}_o^1 + \sigma S_2 \frac{\beta_0\mu(\boldsymbol{n}_o^2 \cdot \boldsymbol{r}_o)^2}{r^4} \boldsymbol{n}_o^2 \right. \\ & \left. + \sigma S_3 \frac{\beta_0\mu(\boldsymbol{n}_o^3 \cdot \boldsymbol{r}_o)^2}{r^4} \boldsymbol{n}_o^3 + \sigma S_4 \frac{\beta_0\mu(\boldsymbol{n}_o^4 \cdot \boldsymbol{r}_o)^2}{r^4} \boldsymbol{n}_o^4 \right] \Big/ \\ & \times [\sigma(S_1 + S_2 + S_3 + S_4) + m_b + m_s + m_p] \end{aligned} \tag{B4}$$

The moment relative to mass center of the sailcraft is given by

$$\boldsymbol{M}_{O_s} = \boldsymbol{r}_{O_sP_1} \times \boldsymbol{F}_b^1 + \boldsymbol{r}_{O_sP_2} \times \boldsymbol{F}_b^2 \tag{B5}$$

where

$$\boldsymbol{F}_b^1 = \sigma S_1 \frac{\beta_0\mu\left(\boldsymbol{n}_b^1 \cdot \boldsymbol{n}_b^s\right)^2}{r^2} \boldsymbol{n}_b^1 + \sigma S_2 \frac{\beta_0\mu\left(\boldsymbol{n}_b^2 \cdot \boldsymbol{n}_b^2\right)^2}{r^2} \boldsymbol{n}_b^2$$

and

$$\boldsymbol{F}_b^2 = \sigma S_3 \frac{\beta_0\mu\left(\boldsymbol{n}_b^3 \cdot \boldsymbol{n}_s^3\right)^2}{r^2} \boldsymbol{n}_b^3 + \sigma S_4 \frac{\beta_0\mu\left(\boldsymbol{n}_b^4 \cdot \boldsymbol{n}_b^s\right)^2}{r^2} \boldsymbol{n}_b^4, \quad \boldsymbol{n}_b^s = A \cdot \boldsymbol{n}_o^s$$

where r is the distance from the sail to the sun; $\boldsymbol{n}_o^s$ is the unit vector of the solar-pressure direction expressed in the orbital frame; and A is the transition matrix from the orbital frame to the body-fixed frame.

The coefficient matrices of the linearized coupled dynamic equation can be obtained as

$$J = \omega_0 \begin{bmatrix} 0 & -2 & 0 \\ 2 & 0 & 0 \\ 0 & 0 & 0 \end{bmatrix} \tag{B6}$$

$$J_1 = \omega_0 \boldsymbol{I}^{-1}(I_z - I_x - I_y)\begin{bmatrix} 0 & 1 & 0 \\ -1 & 0 & 0 \\ 0 & 0 & 0 \end{bmatrix} \tag{B7}$$

$$V = f_r(\boldsymbol{r}_0) + g_r(\boldsymbol{r}_0) - \omega_0^2 \begin{bmatrix} 1 & 0 & 0 \\ 0 & 1 & 0 \\ 0 & 0 & 0 \end{bmatrix} \tag{B8}$$

where

$$f_r = -\frac{\mu}{r^3} I_{3\times 3} + 3\frac{\mu}{r^5}\boldsymbol{r}\boldsymbol{r}^T$$

$$\begin{aligned} g_r = \Big[& 2\sigma S_1 \beta_0 \frac{\mu}{r^4}(\boldsymbol{n}_1 \cdot \boldsymbol{r})\boldsymbol{n}_1\boldsymbol{n}_1^T - 4\sigma S_1 \beta_0 \frac{\mu}{r^6}(\boldsymbol{n}_1 \cdot \boldsymbol{r})^6 \boldsymbol{n}_1 \boldsymbol{r}^T \\ & + 2\sigma S_2 \beta_0 \frac{\mu}{r^4}(\boldsymbol{n}_2 \cdot \boldsymbol{r})\boldsymbol{n}_2\boldsymbol{n}_2^T - 4\sigma S_2 \beta_0 \frac{\mu}{r^6}(\boldsymbol{n}_2 \cdot \boldsymbol{r})^6 \boldsymbol{n}_2 \boldsymbol{r}^T \\ & + 2\sigma S_3 \beta_0 \frac{\mu}{r^4}(\boldsymbol{n}_3 \cdot \boldsymbol{r})\boldsymbol{n}_3\boldsymbol{n}_3^T - 4\sigma S_3 \beta_0 \frac{\mu}{r^6}(\boldsymbol{n}_3 \cdot \boldsymbol{r})^6 \boldsymbol{n}_3 \boldsymbol{r}^T \\ & + 2\sigma S_4 \beta_0 \frac{\mu}{r^4}(\boldsymbol{n}_4 \cdot \boldsymbol{r})\boldsymbol{n}_4\boldsymbol{n}_4^T - 4\sigma S_4 \beta_0 \frac{\mu}{r^6}(\boldsymbol{n}_4 \cdot \boldsymbol{r})^6 \boldsymbol{n}_4 \boldsymbol{r}^T \Big] / \\ & \times [\sigma(S_1 + S_2 + S_3 + S_4) + m_1 + m_2] \end{aligned}$$

$$V_1 = \omega_0^2 \boldsymbol{I}^{-1} \begin{bmatrix} I_z - I_y & 0 & 0 \\ 0 & I_z - I_x & 0 \\ 0 & 0 & 0 \end{bmatrix} + \boldsymbol{I}^{-1}\frac{\partial M_{O_s}}{\partial \boldsymbol{\chi}} \tag{B9}$$

where

$$\frac{\partial M_{O_s}}{\partial \boldsymbol{\chi}} = \boldsymbol{r}_{O_s P_1} \times \frac{\partial \boldsymbol{F}_b^1}{\partial \boldsymbol{\chi}} + \boldsymbol{r}_{O_s P_2} \times \frac{\partial \boldsymbol{F}_b^2}{\partial \boldsymbol{\chi}}, \qquad \frac{\partial \boldsymbol{F}_b^1}{\partial \boldsymbol{\chi}} = \frac{\partial \boldsymbol{F}_b^1}{\partial \boldsymbol{n}_s}\frac{\partial \boldsymbol{n}_b^s}{\partial \boldsymbol{\chi}}$$

$$\frac{\partial \boldsymbol{F}_b^1}{\partial \boldsymbol{n}_b^s} = 2\sigma S_1 \frac{\beta_0 \mu \left(\boldsymbol{n}_b^1 \cdot \boldsymbol{n}_b^s\right)}{r^2}\boldsymbol{n}_b^1 \boldsymbol{n}_b^{1T} + 2\sigma S_2 \frac{\beta_0 \mu \left(\boldsymbol{n}_b^2 \cdot \boldsymbol{n}_b^s\right)}{r^2}\boldsymbol{n}_b^2 \boldsymbol{n}_b^{2T}$$

$$\frac{\partial \boldsymbol{F}_b^2}{\partial \boldsymbol{n}_b^2} = 2\sigma S_3 \frac{\beta_0 \mu \left(\boldsymbol{n}_b^3 \cdot \boldsymbol{n}_b^s\right)}{r^2}\boldsymbol{n}_b^3 \boldsymbol{n}_b^{3T} + 2\sigma S_4 \frac{\beta_0 \mu \left(\boldsymbol{n}_b^4 \cdot \boldsymbol{n}_b^s\right)}{r^2}\boldsymbol{n}_b^4 \boldsymbol{n}_b^{4T}$$

$$\frac{\partial \boldsymbol{n}_b^s}{\partial \boldsymbol{\chi}} = \begin{bmatrix} 0 & -\sin\gamma & 0 \\ \sin\gamma & 0 & -\cos\gamma \\ 0 & \cos\gamma & 0 \end{bmatrix}, \qquad \tan\gamma = \frac{z_0}{\rho_0}$$

$$L = \sum_{i=1}^{4} g_{n_o^i}\frac{\partial \boldsymbol{n}_o^i}{\partial \boldsymbol{\chi}} \tag{B10}$$

where

$$g_{n_o^i} = \sigma S_i \beta_0 \frac{\mu}{r^4}(\boldsymbol{n}_i \cdot \boldsymbol{r})^2 I_{3\times 3} + 2\sigma S_i \beta_0 \frac{\mu}{r^4}(\boldsymbol{n}_i \cdot \boldsymbol{r})\boldsymbol{n}_i \boldsymbol{n}_i^T$$

$$\frac{\partial \boldsymbol{n}_o^i}{\partial \boldsymbol{\chi}} = -\tilde{\boldsymbol{n}}_o^i = -\begin{bmatrix} 0 & -n_o^{i3} & n_o^{i2} \\ n_o^{i3} & 0 & -n_o^{i1} \\ -n_o^{i2} & n_o^{i1} & 0 \end{bmatrix}$$

$$L_1 = \frac{\partial M}{\partial \boldsymbol{r}} = \boldsymbol{r}_{O_s P_1} \times \frac{\partial \boldsymbol{F}_b^1}{\partial \boldsymbol{r}} + \boldsymbol{r}_{O_s P_2} \times \frac{\partial \boldsymbol{F}_b^2}{\partial \boldsymbol{r}} \tag{B11}$$

The unknown derivative items $\partial \boldsymbol{F}_b^i / \partial \boldsymbol{r}$ ($i = 1, 2$) can be obtained according to $\partial \boldsymbol{F}_b^i / \partial \boldsymbol{n}_b^s$ ($i = 1, 2$).

Appendix C: Expressions of the Vectors in the Frames

The normal vectors related to the sailcraft can be expressed in the body-fixed frame as

$$\boldsymbol{n} = [\cos(\gamma + \alpha) \;\; 0 \;\; \sin(\gamma + \alpha)]^T \tag{C1}$$

$$\boldsymbol{n}_1 = [\cos(\gamma - \alpha_1) \;\; 0 \;\; \sin(\gamma - \alpha_1)]^T \tag{C2}$$

$$\boldsymbol{n}_2 = [\cos(\gamma + \alpha_2) \;\; 0 \;\; \sin(\gamma + \alpha_2)]^T \tag{C3}$$

$$\begin{aligned} \boldsymbol{n}_3 = \Bigg[& \cos\frac{\pi - \gamma_1'}{2}\cos\left(\gamma + \alpha_2 + \frac{\gamma_1}{2} - \frac{\pi}{2}\right) \\ & \sin\frac{\pi - \gamma_1'}{2} \quad \cos\frac{\pi - \gamma_1'}{2}\sin\left(\gamma + \alpha_2 + \frac{\gamma_1}{2} - \frac{\pi}{2}\right)\Bigg]^T \end{aligned} \tag{C4}$$

$$\begin{aligned} \boldsymbol{n}_4 = \Bigg[& \cos\frac{\pi - \gamma_1'}{2}\cos\left(\gamma + \alpha_2 + \frac{\gamma_1}{2} - \frac{\pi}{2}\right) \\ & -\sin\frac{\pi - \gamma_1'}{2} \quad \cos\frac{\pi - \gamma_1'}{2}\sin\left(\gamma + \alpha_2 + \frac{\gamma_1}{2} - \frac{\pi}{2}\right)\Bigg]^T \end{aligned} \tag{C5}$$

The pressure center for the resultant force generated by opposed sails can be given by

$$|OP_1| = h_2 \sec\vartheta \tag{C6}$$

$$|OP_2| = \frac{h_3}{\cos(\gamma_1'/2)} \tag{C7}$$

where

$$\vartheta = \tan^{-1}\frac{h_1 - h_2\cos\gamma_1}{h_2\sin\gamma_1}$$

and h_i is the distance from the apex to the mass center of S_i ($i = 1, 2, 3, 4$).

The vectors of the pressure center, relative to point O, can be written as

$$\boldsymbol{r}_{OP_1} = |OP_1|\left[\cos\left(\vartheta + \alpha_2 + \gamma - \frac{\pi}{2}\right) \;\; 0 \;\; \sin\left(\vartheta + \alpha_2 + \gamma - \frac{\pi}{2}\right)\right]^T \tag{C8}$$

$$\boldsymbol{r}_{OP_2} = |OP_2|\left[\cos\left(\gamma + \alpha_2 + \frac{\gamma_1}{2} - \frac{\pi}{2}\right) \;\; 0 \;\; \sin\left(\gamma + \alpha_2 + \frac{\gamma_1}{2} - \frac{\pi}{2}\right)\right] \tag{C9}$$

The mass center of the whole sailcraft can be obtained by integrating the system

$$\boldsymbol{r}_{OO_s} = \frac{\int r\,\mathrm{d}m}{[\sigma(S_1 + S_1 + S_3 + S_4) + m_s + m_p + m_b]} \tag{C10}$$

where $\boldsymbol{r}$ is the vector of the mass point relative to point O.

Then, the vectors of the pressure center, relative to the mass center of the sailcraft, can be obtained as

$$\boldsymbol{r}_{O_s P_1} = \boldsymbol{r}_{OP_1} - \boldsymbol{r}_{OO_s} \tag{C11}$$

$$\boldsymbol{r}_{O_s P_2} = \boldsymbol{r}_{OP_2} - \boldsymbol{r}_{OO_s} \tag{C12}$$

The solar light vector can be expressed in the orbital frame as

$$\boldsymbol{n}_s = \boldsymbol{r}_1/r_1 = [\cos\gamma \quad 0 \quad \sin\gamma]^T \tag{C13}$$

where $\tan\gamma = z_0/\rho_0$, $\boldsymbol{r}_0 = [\rho_0 \quad 0 \quad z_0]^T$.

Acknowledgments

This work was supported by the National Natural Science Foundation of China (Grants No. 10602027 and No. 10672084). The authors would like to acknowledge Janice Willson for meticulous revision of the paper.

References

[1] West, J. L., "NOAA/DOD/NASA Geostorm Warning Mission," Jet Propulsion Lab, California Institute of Technology, JPL D-13986, Pasadena, CA, Oct. 1996.
[2] Prado, J. Y., Perret, A., Pignolet, G., and Dandouras, I., "Using a Solar Sail for a Plasma Storm Early Warning System," International Academy of Astronautics, Paper 96-IAA. 3.3.06, Oct. 1996.
[3] Forward, R. L., "Light-Levitated Geostationary Cylindrical Orbits," *Journal of the Astronautical Sciences*, Vol. 29, No. 1, 1981, pp. 73–80.
[4] McInnes, C. R., and Simmons, F. L., "Solar Sail Halo Orbits 1: Heliocentric Case," *Journal of Spacecraft and Rockets*, Vol. 29, No. 4, 1992, pp. 466–471.
[5] McInnes, C. R., "Non-Keplerian Orbits for Mars Solar Reflectors," *Journal of the British Interplanetary Society*, Vol. 55, Nos. 3–4, 2002, pp. 74–82.
[6] McInnes, C. R., "Passive Control of Displaced Solar Sail Orbits," *Journal of Guidance, Control, and Dynamics*, Vol. 21, No. 6, 1998, pp. 975–982.
[7] McInnes, C. R., and Macpherson, K. P., "Solar Sail Halo Trajectories: Dynamics and Applications," 42nd International Astronautical Congress, Vol. 1, Montreal, IAF-91-334, 1991, pp. 5–11.
[8] McInnes, C. R., "Solar Sail Mission Applications for Non-Keplerian Orbits," *Acta Astronautica*, Vol. 45, Nos. 4–9, 1999, pp. 567–575.
[9] McInnes, C. R., and Simmons, F. L., "Solar Sail Halo Orbits 2: Geocentric Case," *Journal of Spacecraft and Rockets*, Vol. 29, No. 4, 1992, pp. 462–479.
[10] Molostov, A. A., and Shvartsburg, A. A., "Heliocentric Halos for a Solar Sail with Absorption," *Soviet Physics Dokladv*, Vol. 37, No. 3, 1992, pp. 149–152.
[11] Molostov, A. A., and Shvartsburg, A. A., "Heliocentric Synchronous Halos for a Solar Sail with Absorption," *Soviet Physics Doklady*, Vol. 37, No. 4, 1992, pp. 195–197.
[12] Sohn, R. L., "Attitude Stabilization by Means of Solar Radiation Pressure," *ARS Journal*, Vol. 29, May 1959, pp. 371–373.
[13] Benjamin, L. D., "Attitude Control and Dynamics of Solar Sails," M.S. Thesis, Aeronautics and Astronautics Department, Univ. of Washington, Seattle, WA, 2001.
[14] Wie, B., "Solar Sail Attitude Control and Dynamics, Part 1," *Journal of Guidance, Control, and Dynamics*, Vol. 27, No. 4, 2004, pp. 526–535.
[15] Wie, B., "Solar Sail Attitude Control and Dynamics, Part 2," *Journal of Guidance, Control, and Dynamics*, Vol. 27, No. 4, 2004, pp. 536–544.
[16] Wie, B., and David, M., "Robust Attitude Control Systems Design for Solar Sail, Part 1: Proellantless Primary ACS," *AIAA Guidance, Navigation, and Control Conference and Exhibit*, Vol. 1, AIAA, Reston, VA, 2004, pp. 1–28.
[17] Acord, J. D., and Nicklas, J. C., "Theoretical and Practical Aspects of Solar Pressure Attitude Control for Interplanetary Spacecraft," *Guidance and Control 2*, Vol. 13, Progress in Astronautics and Aeronautics, Academic Press, New York, 1964, pp. 73–101.

C. Kluever
Associate Editor